Design of Multifunctional Structural Battery Composites for the Next Generation of Electric Vehicles

SAMAN FARHANGDOUST[1*], SHABBIR AHMED[1], ALEXANDER STRANGE[1], UMUT ALTUNTAS[1], CHAOQUN DUAN[1], YAQOUB ABDULLAH[1], FRANKLIN LI[2], SERENA WANG[2] and FU-KUO CHANG[1]

ABSTRACT

A multifunctional energy storage composite (MESC) combines the high energy density of lithium-ion batteries with the structural benefits of carbon fiber composites, resulting in a lightweight structural battery with excellent mechanical strength and enhanced safety for electric vehicles (EVs). This paper presents the design-to-fabrication development of new MESC, with a specific focus on the design, fabrication, and testing of an electronic skateboard (e-skateboard) as a representative system-level study for the EVs. A finite element analysis (FEA) is employed to design the MESC e-skateboard. The FEA of the MESC e-skateboard is validated through mechanical testing, demonstrating a significant 24% reduction in weight, leading to an impressive 31.6% improvement in energy density compared to a conventional e-skateboard. As a part of the MESC technology, an embedded smart sensor network is also developed for the e-skateboard, showcasing the capability for real-time battery monitoring, and estimating its state of charge during in-service operation. The promising outcomes of the new MESC technology position it as a novel solution for enabling multifunctional structural battery composites in future electronic vehicles and aircraft applications.

INTRODUCTION

In recent years, there has been exponential growth in the use of lithium-ion structural batteries in electronic vehicles (EV), driven by their high energy density and long endurance life [1-2]. While different research groups and companies have attempted various strategies to incorporate lithium-ion battery technology into the structural components of electric vehicles, there is often a compromise between two main design objectives: energy density and mechanical strength. Due to the susceptibility of lithium-ion batteries to environmental conditions such as impact, the inclusion of additional supporting structures is necessary to protect such these combustible batteries. However,

*Corresponding Author: sfarhang@stanford.edu
[1]Structures and Composites Laboratory (SACL), Aeronautics and Astronautics Department, Stanford University, Stanford, CA 94305, U.S.A.
[2]Acellent Technologies Inc., 835 Stewart Dr, Sunnyvale, CA 94085, USA.

the battery protections result in increased weight for EV and subsequently reduce their energy efficiency [3]. Therefore, developing a lightweight structural battery with high energy density and excellent mechanical strength is crucial.

By integrating three subsystems - energy storage, structure, and health monitoring - into a single multifunctional system, the Stanford Structures and Composites Laboratory (SACL) developed a multifunctional energy storage composite (MESC) technology [5-6]. The MESC provides a self-sufficient structural battery, capable of supporting the structural loads of the overall system. It involves sandwiching a lithium-ion battery between two thin composite face sheets, wherein a polyethylene polymer frame is employed to seal the battery's electrolytes. Additionally, polymer material is used to bridge the interior surface of the two composite face sheets, creating a mechanical bond between the battery and the carbon fiber encapsulation [6-7].

As an improvement on the MESC design, this paper introduces a new multifunctional structural battery composite that replaces the bulky and heavy polyethylene frame with a lightweight pouch bag for battery isolation, thereby improving the overall energy density efficiency. To achieve this, a FEA is conducted to assess the performance of the MESC e-skateboard under varying distributed loads. Additionally, experimental tests are carried out to validate the feasibility of the MESC concept. The MESC not only offers a good mechanical strength to protect batteries but also reduces system weight by eliminating the need for conventional battery protection. which is an invaluable resource for researchers and engineers involved in the field of energy storage composite and structural battery technology.

METHOD OF APPROACH

In this paper, we present the design-to-fabrication process of MESC for electric vehicle applications. This process aims to efficiently support desired loads, store sufficient energy, reduce overall structural weight, and ultimately enhance energy density at the system level. As depicted in Figure 1, the process involves three key steps: 1) Finite element analysis and design, 2) Integrated manufacturing process, and 3) Real-time monitoring for battery and structural health.

We developed the design-to-manufacturing process of the MESC approach for an e-skateboard, as a quintessential example of EV. As we delve into the realm of EVs, an e-skateboard will serve as a system-level case study, offering valuable insights into the innovative possibilities and potential improvements in the field of structural battery for the EV applications.

In conventional e-skateboards, batteries are typically positioned on the bottom of the deck, protected by a separate enclosure, which adds extra weight and reduces overall efficiency of the e-skateboards. As an advanced alternative, the MESC approach seamlessly integrates the batteries into the entire deck structure, eliminating the need for additional enclosures. By replacing the conventional deck with the MESC deck, the system's overall weight is significantly reduced, leading to improved energy density and efficiency. For the proposed MESC approach, an embedded smart sensor networks are also implemented into the MESC deck to monitor battery reliability and estimate their state of charge (SoC) in real-time during operation.

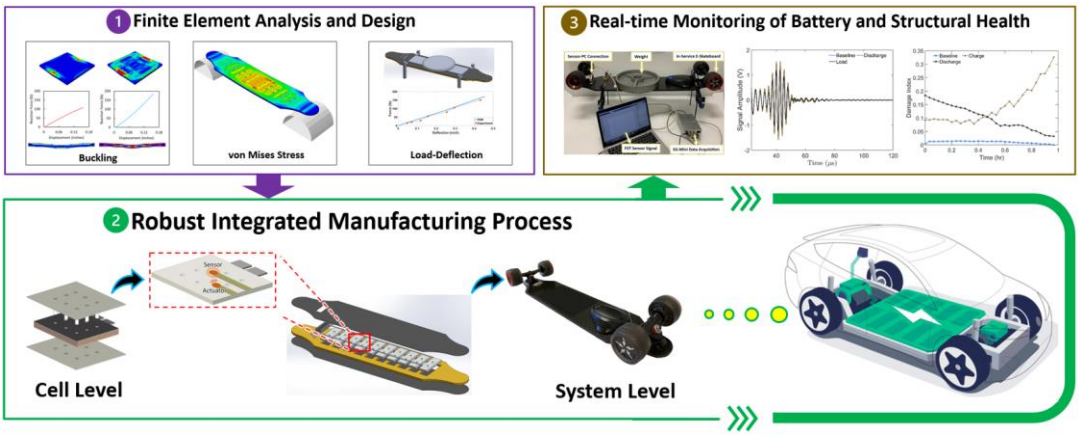

Figure 1. The Design-to-Fabrication process of the MESC

DESIGN

The proposed MESC deck consists of core foam and two high-strength CFRP composite face sheets that are integrated with lithium-ion battery pouch cells using epoxy (Figure 2). To further strengthen the mechanical bond between the battery and the CFRP encapsulation, epoxy material is injected through the thickness of the polymer reinforcements. Indeed, one of the key components of the MESC deck is the utilization of polymer reinforcements (e.g., polyethylene spacers) to create a bridge between two face sheets of the sandwich composites and facilitate load transfer through lithium-ion battery pouch cells. These spacers also play an important role to enhance the stiffness and strength of the MESC pouch cells. The MESC design enables interlocking of the layers within the battery stack, resulting in improved structural integrity and stability. By incorporating mechanical robustness directly into the cells, significant weight reduction can be attained. This approach aims to optimize the energy density efficiency of the e-skateboard and simultaneously preserve the mechanical strength performance of its pouch Li-ion batteries.

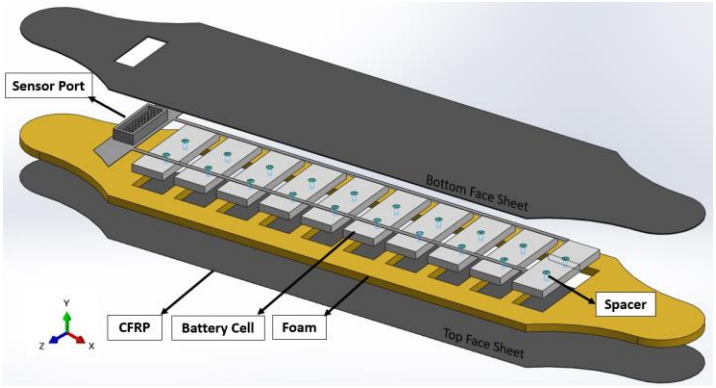

Figure 2. The MESC E-skateboard in detail

.

Commercial E-skateboards have a 11-15 miles range and 90-250 Wh energy capacity. Based on the commercial study of available electric skateboards, the objective was to design an e-skateboard with 1.3-mile range and 133 Wh energy capacity. To

achieve this, we utilized 10 Lithium-ion pouch cells, each with a charge capacity of 3.6 Ah and a voltage of 3.7 V. Table I presents the electrical metrics of the MESC e-skateboard.

TABLE I. ELECTRICAL METRICS OF THE MESC E-SKATEBOARD

Characteristics	Value
Number of cells	10 Cells
Charge Capacity of each cell	3.6 Ah
Charge Capacity of whole system	3.6 Ah
Current Supplied	1.14 A
Battery Charging Time [Charge Capacity /Current Supplied]	3.2 h
Voltage of each cell	3.7 V
Voltage of whole system	37 V
Energy Capacity [Charge Capacity*Voltage]	133 Wh
Range [(Energy Capacity *Efficiency Coefficient)/ (Average Wh per mile)]	13.3 miles

The normal size for commercial e-skateboards can vary depending on the brand, model, and intended use. However, most commercial e-skateboards typically fall within the range of 32 to 42 inches in length and 8 to 10 inches in width. These dimensions are similar to standard skateboard sizes and are designed to provide a balance between maneuverability and stability. Consequently, for the deck of the proposed MESC e-skateboard, dimensions of 0.43 inches for thickness, 8.27 inches for width, and 39.18 inches for length were selected. Figure 3 depicts the dimensions of the MESC e-skateboard.

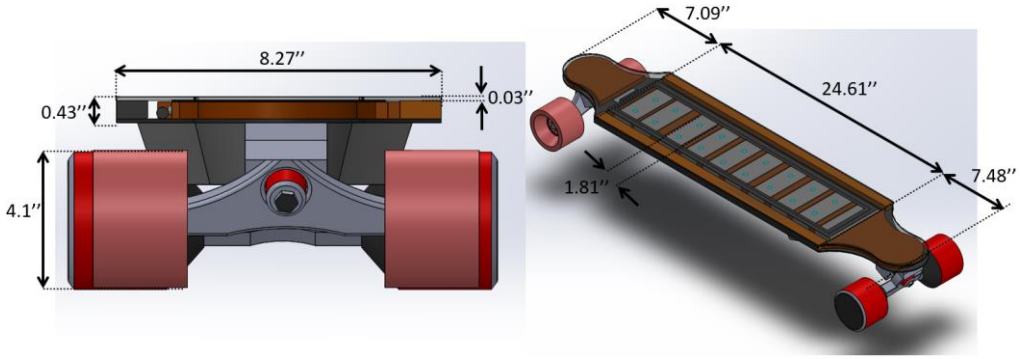

Figure 3. The size and dimensions of the MESC E-skateboard.

FINITE ELEMENT ANALYSIS

To investigate the mechanical performance of the proposed MESC design, finite element analysis (FEA) using Abaqus was employed to simulate the 3D models of two e-skateboards: one with a conventional deck and one with the MESC deck. The validation of the MESC e-skateboard simulation was carried out using experimental results, accordingly. In the simulation, a distributed load of 200lb was applied to the upper surface of the skateboards and two rigid circular rollers were modeled to represent the boundary conditions. These rollers were fixed in all directions. Friction and hard

contact were introduced between the roller's surface and the bottom surface of the skateboards. Additionally, tie contact was defined between the foam-CFRP, CFRP-epoxy, epoxy-polymer, and polymer battery interfaces. Frictional-hard contact was used for the battery-CFRP and battery-foam surfaces. The mesh size was set to 6 mm for CFRP, foam, and battery, and 1 mm for epoxy. During the mesh convergence analysis, it was observed that reducing the mesh size of the CFRP to 4 mm increased the maximum stress by 9% (which is below the 10% threshold). Therefore, a mesh size of 6 mm was determined as suitable for achieving mesh convergence. Table II displays the material properties of the finite element models.

TABLE II. MATERIAL PROPERTIES OF SIMULATION MODELS

Material	Property	Value
Epoxy	Elastic modulus	3350 (MPa)
	Poisson's ratio	0.3
Foam	Elastic modulus	42 (MPa)
	Poisson's ratio	0.3
Battery	Elastic modulus	80 (MPa)
	Poisson's ratio	0.3
Composite	E1, E2	135GPa
	E3	9.2GPa
	Poisson's ratio	0.3
	G12	10.4GPa
	G23, G13	4.5GPa

As a proof of the MESC approach, the distribution of von Mises stress clearly illustrates that the polymer reinforcement occurs at the contact between the polymer reinforcements and CFRP face sheets. This emphasizes the critical role of the polymer reinforcement in bearing the applied load and effectively transferring it through the battery, ensuring minimal stress on the battery pouch cells (Figure 4).

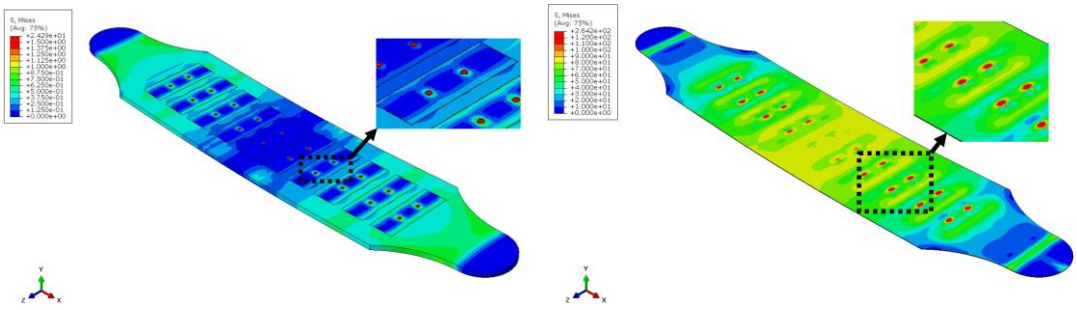

Figure 4. The von Mises stress distribution of foam, battery, and reinforcement polymers in the middle of the MESC E-skateboard (left). The von Mises stress distribution at the contact between the polymer reinforcements and bottom CFRP face sheet of the MESC E-skateboard.

The deflection of the sandwich composite deck can be obtained from the Elementary Sandwich Theory as

$$\delta = \frac{PL^3}{48EI_{yy}} + \frac{PL}{4GA} \quad (1)$$

In which, EI_{yy}, G, A, P, and L denote bending stiffness, shear modulus, the cross-sectional area of the foam, applied load, and the length of deck, respectively. Assuming the shear deformation in the composite face sheets is negligible, we can use Eq. (2) to calculate the bending stiffness (EI_{yy}).

$$EI_{yy} = \frac{PL^3}{48\delta} \quad (2)$$

As demonstrated in the force-deflection curve (Figure 5), the MESC e-skateboard achieves a deflection of 0.67 inches under a 200 lb load, meeting the standard design requirement for a typical skateboard (<0.9 inches) [6]. Furthermore, the FEA results confirm that the MESC e-skateboard can achieve a bending stiffness of 33,266 lb/inches under a 200 lb load, which is comparable to the conventional e-skateboard's bending stiffness of 36,143 lb/inches.

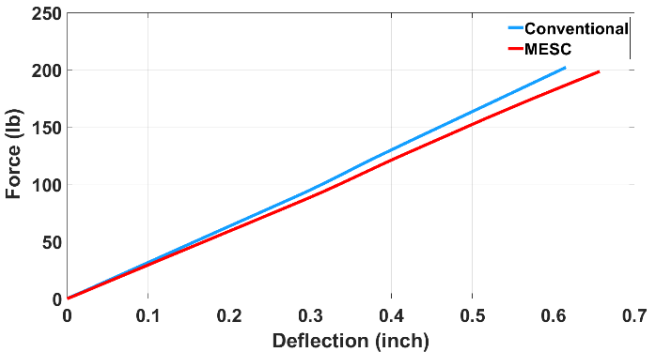

Sample	Stiffness at 200 lb
Conventional	36143 (lb./inch)
MESC based	33266 (lb./inch)

Figure 5. Force against deflection curve for conventional and MESC e-skateboards.

FABRICATION

Based on the MESC e-skateboard design from the simulation part, the fabrication process starts with producing 10 lithium-ion pouch cells to reach the 133 Wh design goal. The fabrication is divided into two stages: MESC pouch cell and MESC E-skateboard fabrication (Figure 6). As the MESC features a polymer spacer inside the pouch bag, the fabrication process of the MESC pouch cell necessitates certain modifications compared to traditional battery fabrication methods. After injecting the bag with electrolytes and sealing the pouch bag, the cells are connected to a Cycler to undergo the formation process. In the final step, all battery cells undergo the degassing process and are subsequently resealed. To assess their electrical performance in cycling and HPPC tests, all cells are connected to the Cycler for measurement and analysis.

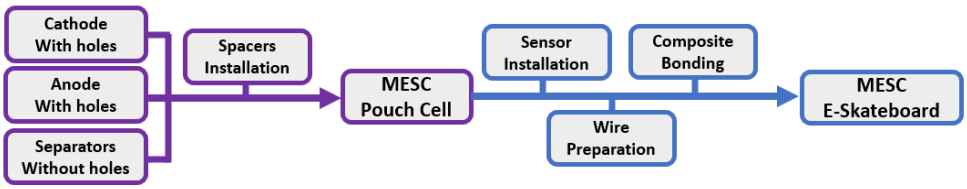

Figure 6. The cell-level (purple) and system-level (blue) fabrication process for the MESC.

To fabricate the MESC deck, the 10 battery pouch cells are sandwiched between two CFRP face sheets. The composite sheets are constructed using plies of 0/90 weave. The tabs of the cells are connected using wires in a series configuration, and the status of the cells is monitored using a Battery Management System (BMS). Epoxy is employed to bond the polymer spacer and foams to the two CFRP face sheets. Subsequently, a smart sensor layer is installed on the second surface of the cells. The sensor data helps to monitor the health of the battery cells and estimate the battery state of charge for the MESC e-skateboard. Figure 7 provides detailed information about the deck's structure of the MESC e-skateboard.

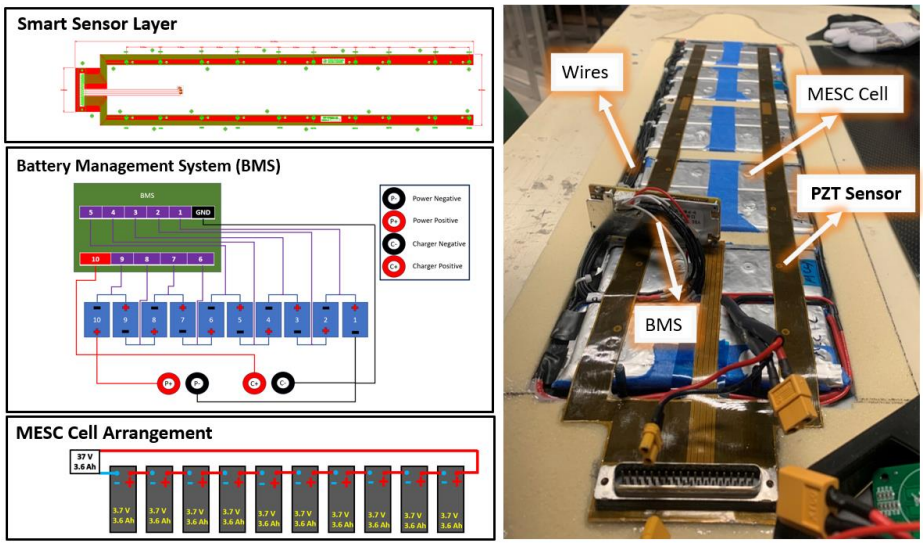

Figure 7. The schematic of the smart sensor layer and BMS (left), and a picture of the inside of the MESC e-skateboard during the fabrication process (right).

EXPERIMENTAL VALIDATION

One of the objectives in this research was to optimize the specific energy by replacing the battery enclosure and deck with a structural battery deck, maximizing its potential. Figure 8 provides a comparison between the final product of the MESC e-skateboard and a conventional e-skateboard.

Figure 8. Commercial E-skateboard (left) and MESC E-skateboard (right).

Both skateboards have the same energy capacity of 133.2 Wh. However, the MESC e-skateboard eliminates the need for a separate battery enclosure, resulting in a weight reduction of 24%. Consequently, the MESC e-skateboard achieves a 31.6% improvement in energy density (Table III).

TABLE III. RANGE OF SAVING WEIGHT BY MESC METHOD

Properties	**MESC**	**Convention e-skateboard [6]**
Max Load	150 kg	150 kg
Max Speed	30 mph	30 mph
Total Skateboard Weight	8.5 kg	8.1 kg
Electrical Module (BMS and Wires)	0.45 kg	0.45 kg
Battery Pack Weight	0 kg	1.34 kg
Deck Weight	2.85 kg	3.75 kg
Save Weight	**24 %**	
Energy Capacity	133.2 Wh	133.2 Wh
Energy Density	46.6 Wh/Kg	35.4 Wh/Kg
Energy Efficiency	**31.6 %**	

As depicted in Figure 9, the simulation model was validated through a three-point bending test conducted on the MESC deck. Different weights were manually added and balanced to measure the deflection values at the midspan (directly under the applied load). The results of the test perfectly align with the output of the simulation model in midpoint deflection.

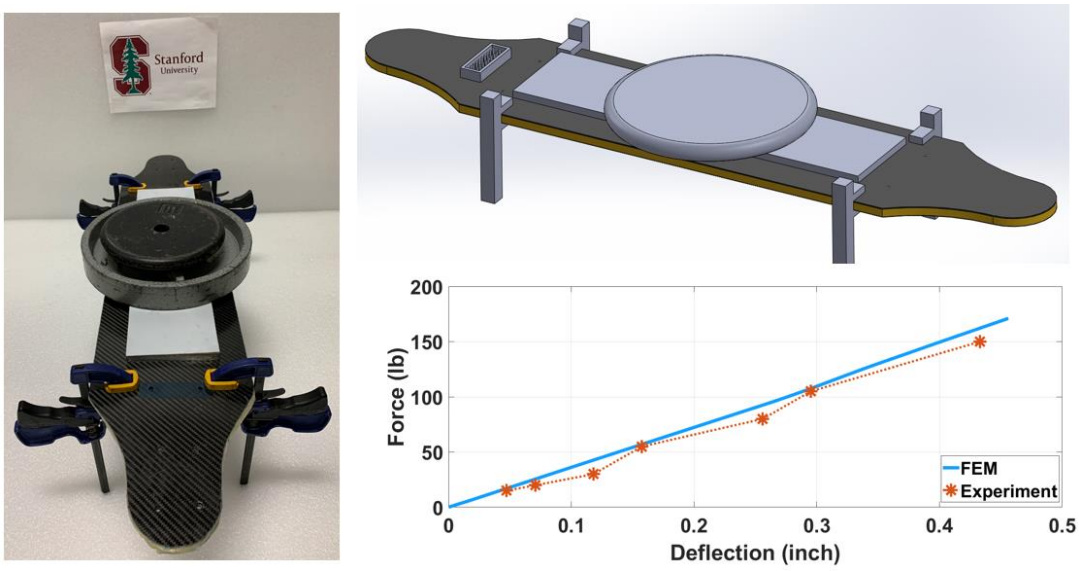

Figure 9. The fabrication process for MESC Pouch Cell.

REAL-TIME MONITORING

To demonstrate the real-time monitoring capability of the MESC e-skateboard, a smart layer sensor was integrated into the deck, specifically on the surface of the battery cells. Utilizing piezoelectric sensors, ultrasonic guided wave signals were captured from

the MESC e-skateboard under three distinct conditions: baseline, discharge, and load. In the baseline condition, the skateboard was at rest, the batteries were neither charging nor discharging, and no load was applied. For the discharge condition, the e-skateboard wheels were continuously turned, while ultrasonic signals were simultaneously collected. Finally, a 25 lb load was applied to the e-skateboard, and ultrasonic signals were acquired (Figure 10).

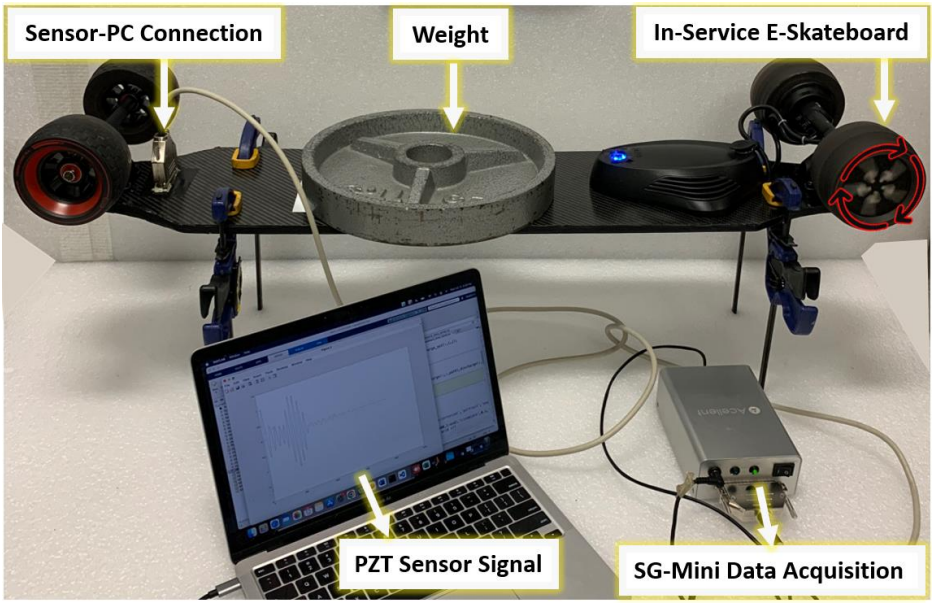

Figure 10. The experimental setup to collect sensor data from battery cells of the MESC e-skateboard while the deck was subjected to a 25 lb load.

Figure 11 shows that the ultrasonic signals exhibit significant change during the discharge phase, whereas, there is minimal change in the signal for the baseline and load conditions. This observation indicates that the integrity of the battery is not affected by the application of load. This can be attributed to the load transfer capability of the MESC pouch cell, facilitated by the reinforced polymer used in its construction.

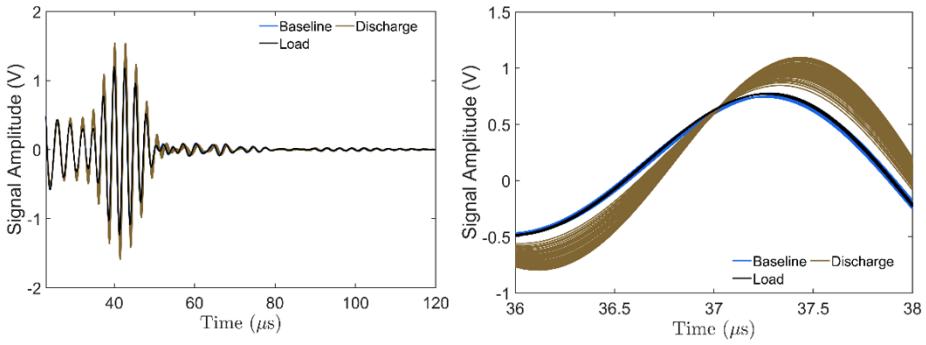

Figure 11. Ultrasonic guided wave signals collected from the MESC e-skateboard under different conditions: baseline, discharge, and load, showcasing the full signal (left) and a zoomed-in view (right).

Figure 12 (left-top) displays the voltage and current profiles of a lithium-ion pouch cell used in the MESC e-skateboard for a C/3 charge and discharge rate. Simultaneously,

ultrasonic signals were collected during the charge and discharge phases, and a damage index (DI) was derived from these signals. Notably, Figure 12 illustrates that when the SoC reaches 100% at 3 hours (left-top), the damage index reaches its maximum value at the same time (left-bottom). This establishes a direct correlation between the damage index and the state of charge of the battery cell. To demonstrate this concept of SoC estimation on the MESC e-skateboard, using ultrasonic guided waves, thirty guided wave signals were collected at two-minute intervals during the baseline, charge, and discharge conditions from the MESC e-skateboard (Figure 12-right). Then damage indices were obtained from the guided wave signals. The results indicate that the DI remains relatively constant during the baseline phase, while it gradually increases during charging and decreases during discharge. As a result, with proper calibration of the DI, it becomes possible to obtain accurate estimations of the batteries' SoC for the MESC e-skateboard using only the ultrasonic signals.

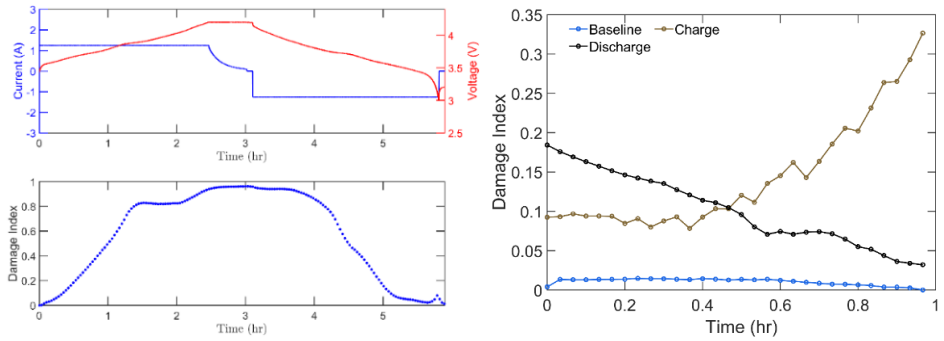

Figure 12. Batteries' SoC estimation for the MESC e-skateboard using Ultrasonic-based DI.

CONCLUSION

This research study successfully demonstrated the capability of the MESC approach for a system-level structural battery application. For the proposed MESC e-skateboard, a remarkable 24% reduction in weight was achieved, resulting in a notable increase in specific energy by 31.6%. This improvement was primarily attributed to the elimination of unnecessary battery cell enclosures. Furthermore, finite element method and experimental analyses demonstrated that the load-transfer capability of the MESC pouch cell can enhance the mechanical performance of the MESC e-skateboard. Another noteworthy aspect of the MESC technology is the integration of in-situ smart sensing systems, which showed the capability for real-time battery monitoring in-service operation. The promising outcomes of the MESC technology position it as a potential solution for enabling structural batteries in future electronic vehicles and aircraft applications.

ACKNOWLEDGEMENT

This work was supported by the Advanced Research Projects Agency – Energy (U.S. Department of Energy) [grant number DE-AR0001151] and our industry partners: Airbus, Embraer, Dassault Systemes, Acellent Technologies, Marubeni, Technologies Renewable Energy Test Center, and Amprius Technologies. We would like to thank

Acellent Technologies for their support in providing the SMART layers. We would also like to thank Stanford Summer Interns: Kyungmin Inn, Joshua Liao, and Ryan Liu for their efforts in sketching and preparing experimental setup.

REFERENCES

1. Grey, C. P., & Hall, D. S. (2020). Prospects for lithium-ion batteries and beyond—a 2030 vision. Nature Communications, 11(1). 4
2. Bravo Diaz, L., He, X., Hu, Z., Restuccia, F., Marinescu, M., Barreras, J. V., Patel, Y., Offer, G., & Rein, G. (2020). Review—meta-review of fire safety of lithium-ion batteries: Industry Challenges and Research Contributions. Journal of The Electrochemical Society, 167(9), 090559.
3. Asp, L. E., Johansson, M., Lindbergh, G., Xu, J., & Zenkert, D. (2019). Structural Battery Composites: A Review. Functional Composites and Structures, 1(4), 042001.
4. Ladpli, P., Nardari, R., Kopsaftopoulos, F., & Chang, F. K. (2019). Multifunctional energy storage composite structures with embedded lithium-ion batteries. Journal of Power Sources, 414, 517-529.
5. Ladpli, P., Kopsaftopoulos, F., & Chang, F. K. (2018). Estimating state of charge and health of lithium-ion batteries with guided waves using built-in piezoelectric sensors/actuators. Journal of Power Sources, 384, 342-354.
6. Ladpli, P., Nardari, R., Liu, H., Slater, M., Kepler, K., Wang, Y., … & Chang, F. K. (2016). Multitfunctional Energy Storage Composites—Electrochemical and Mechanical Cycling Characterization. In Proceedings of the Battery Congress (pp. 1-12).
7. Ladpli, P., Nardari, R., Rewari, R., Liu, H., Slater, M., Kepler, K., ... & Chang, F. K. (2016, June). Multifunctional energy storage composites: design, fabrication, and experimental characterization. In Energy Sustainability (Vol. 50237, p. V002T01A004). American Society of Mechanical Engineers.
8. Fajardo, N. (1919). Modular Electric Skateboard (Doctoral dissertation, Worcester Polytechnic Institute).